Materials Chemistry and Physics 170 (2016) 123–128

Contents lists available at ScienceDirect

Materials Chemistry and Physics

journal homepage: www.elsevier.com/locate/matchemphys

# Micron-size superparamagnetic iron-oxides watercress with unique MRI properties

Wei Liu [1], Ji Ma [1], Kezheng Chen*

*Lab of Functional and Biomedical Nanomaterials, College of Materials Science and Engineering, Qingdao University of Science and Technology, Qingdao 266042, China*

## HIGHLIGHTS

- Micron-size iron oxides exhibit peculiar superparamagnetism.
- Micron-size iron oxides have high $r_2/r_1$ ratio of ca. 20.
- Micron-size iron oxides can be used as $T_2$ contrast agents after surface modification.

## ARTICLE INFO

*Article history:*
Received 27 May 2015
Received in revised form
23 October 2015
Accepted 19 December 2015
Available online 25 December 2015

*Keywords:*
Composite materials
Magnetic materials
Magnetic properties
Biomaterials

## ABSTRACT

In this work, 10-μm-sized superparamagnetic $Fe_3O_4$@(α, γ)–$Fe_2O_3$ watercress was synthesized by a one-step solvothermal method. Meanwhile, the other two kinds of micron-size hierarchical structures were also obtained by solely altering $Fe^{2+}$/urea molar ratio in the same solvothermal procedure. It was found that the nuance of reaction parameters during synthesis can greatly alter the morphologies and structures of the obtained products, but it cannot alter their unique superparamagnetic properties at room temperature. Moreover, these large-size $Fe_3O_4$@(α, γ)–$Fe_2O_3$ products unexceptionally exhibit novel superparamagnetic–ferromagnetic transition around 30 K, indicating that the magnetic arrangement of $Fe_3O_4$ and (α, γ)–$Fe_2O_3$ components in these architectures are virtually the same. These micron-size iron oxides can beat the superparamagnetic size-limit (25–30 nm) of commonly-used $Fe_3O_4$ contrast agents in MRI application.



## 1. Introduction

Naturally ferrimagnetic (FIM) magnetite, $Fe_3O_4$, is an iron oxide polymorph appealing for a variety of applications [1–3] because bulk $Fe_3O_4$ exhibits a high Curie temperature ($T_C^{bulk} = 840$ K) and the highest saturation magnetization ($M_S^{bulk} = 98$ emu/g) among iron oxides [4]. The magnetic behavior of $Fe_3O_4$ is predominantly determined by the size of the particles. When the size reduces to 25–30 nm, $Fe_3O_4$ nanoparticles (NPs) turn into superparamagnetic (SPM) state at room temperature as a consequence of the spontaneous flip of their magnetization due to strong thermal agitation [5]. SPM $Fe_3O_4$ NPs do not retain any permanent magnetization after removal of an applied magnetic field, and thus they are particularly desirable for preparing colloidally stable dispersions because larger FIM $Fe_3O_4$ particles exhibit remanence and coercivity that cause aggregation under a magnetic field.

Although colloidally stable SPM $Fe_3O_4$ NPs have been widely used in a variety of biological applications [6–8], many issues including how to break size limit and enhance magnetic response are still being intensively studied for further improvement. Especially, the ideal particle size for $Fe_3O_4$ contrast agents in MRI diagnosis usually exceeds its superparamagnetic limit (i.e., 25–30 nm) [9]. Further increasing the size of SPM $Fe_3O_4$ NPs would induce the SPM-ferromagnetic (FM) transition, so that these NPs are no longer well-dispersible in solution.

To tackle this issue, many efforts have been devoted to synthesize antiferromagnetic (AFM) NPs that do not suffer from the size limitations SPM NPs encounter [10,11]. However, AFM NPs have low magnetization per particle, so that it is difficult to effectively separate them from solution or control their movement in blood by using moderate magnetic fields. Even worse is the non-negligible remanence and coercivity that are induced by inevitable defects

* Corresponding author.
*E-mail address:* kchen@qust.edu.cn (K. Chen).
[1] These authors contributed equally to this study.

http://dx.doi.org/10.1016/j.matchemphys.2015.12.029
0254-0584/

in AFM lattices, so that their dispersity is poor under an applied magnetic field. These aspects greatly limit their usage in practical applications such as separation and targeted delivery.

In this work, we develop a facile method for the preparation of a micron-size SPM $Fe_3O_4$@(α, γ)−$Fe_2O_3$ watercress-like structure by a solvothermal procedure. The formation of this superstructure is believed to be related to an ethylene glycol (EG)-mediated self-assembly process. These micron-size SPM iron oxides can overcome the size limit of conventional SPM $Fe_3O_4$ contrast agents, and they may be more appropriate for potential contrast enhancers in MRI application.

## 2. Experimental

### 2.1. Synthesis of $Fe_3O_4$@α−$Fe_2O_3$ watercress

Analytical ferrous chloride tetrahydrate ($FeCl_2 \cdot 4H_2O$), urea ($CH_4N_2O$) and EG were purchased from Sinopharm Chemical Reagent Co., Ltd. (China), and used as received without further purification. In a typical synthesis, $FeCl_2 \cdot 4H_2O$ and urea with a molar ratio of 1:1 were dissolved and stirred in 50 mL of EG at room temperature until a homogeneous solution was formed. Then the mixture was transferred into a Teflon-lined stainless-steel autoclave with a capacity of 100 mL for solvothermal treatment at 160 °C for 12 h. The as-obtained precipitate was repeatedly washed with deionized water and ethanol, and finally dried at 60 °C for 6 h.

### 2.2. Characterization

The XRD patterns were recorded on a powder X-ray diffractometer (Rigaku D/max-rA; Japan) equipped with a rotating anode and a Cu -$K_{\alpha 1}$ radiation source (λ = 1.5406 Å) at a step width of 0.02°. The Raman spectrum was recorded using a Super LabRam microscopic Raman spectrometer (Labram, Jobin Yvon, France, a He−Ne laser with an excitation wavelength of 532 nm). Scanning electron microscope (SEM) images were collected on a field -emission scanning electron microscope (JEOL JSM-6700F, Japan). Transmission -electron microscope (TEM) images were performed on the JEOL 2010 TEM (Japan) with an operating voltage of 200 kV. The high-resolution transmission -electron microscope (HRTEM) experiments were conducted using a Field Emission Gun (FEG) JEOL 2010F microscope (Japan) with a point resolution of 0.19 nm. Dynamic light scattering (DLS, Zetasizer Nano, Malvern Instrument) was used to determine zeta potential value of the sample. Magnetic measurements were carried out using a commercial superconducting quantum interference device magnetometer (SQUID MPMS-XL5, U.S.A).

### 2.3. Relaxivity measurements

Proton transverse ($r_2$) and longitudinal ($r_1$) relaxivities of the samples were measured in deionized water at 37 °C using a mq-60 NMR analyzer (Bruker Minispec) at a magnetic field strength of 1.41 T ($\omega_0 = 60$ MHz). $T_2$ relaxation times were obtained from fitting a monoexponential decay curve to signal data generated by a Carr−Purcell−Meiboom−Gill (CPMG) spin-echo pulse sequence with an interecho time of 1 m and repetition time of 17.5 s. $T_1$ relaxation times were obtained from fitting a monoexponential recovery curve to signal data generated with an inversion recovery (IR) pulse sequence using 10 inversion times between 0.05 and 15 s. The relaxivities $r_1$ and $r_2$ were determined from the slopes of the straight lines on a graph of the respective relaxation rate ($s^{-1}$) versus iron concentration (mmol $L^{-1}$ Fe). Iron concentrations were determined by inductively coupled plasma-optical emission spectrometer (ICP-OES, Perkin−Elmer, Optima 8000).

## 3. Results and discussion

The chemical composition of the 12 h-product is shown in Fig. 1(a). The broad peak widths and low peak intensities indicate the as-prepared product is poorly crystallized, and the main diffraction peaks in the pattern are seemingly identical with the standard card of $Fe_3O_4$ (JCPDS No. 85-1436), γ−$Fe_2O_3$ (JCPDS No. 39-1346) and α−$Fe_2O_3$ (JCPDS No. 85-0599). Further, a Raman spectrum was measured to validate the composition of the product. In Fig. 1(b), the 215, 389 and 585 $cm^{-1}$ Raman scattering peaks are characteristically assigned to $A_{1g}$ mode of α−$Fe_2O_3$, $T_{2g}$ mode of γ−$Fe_2O_3$ and $T_{2g}$ mode of $Fe_3O_4$, respectively [12,13]. The intense feature at 1281 $cm^{-1}$ is derived from α−$Fe_2O_3$ phonon scattering [14]. The 277 $cm^{-1}$ band is assigned to $T_{2g}$ mode of $Fe_3O_4$ and/or $E_g$ mode of α−$Fe_2O_3$. The 489 $cm^{-1}$ band is assigned to $T_{2g}$ mode of γ−$Fe_2O_3$ and/or $A_{1g}$ mode of α−$Fe_2O_3$. These Raman scattering

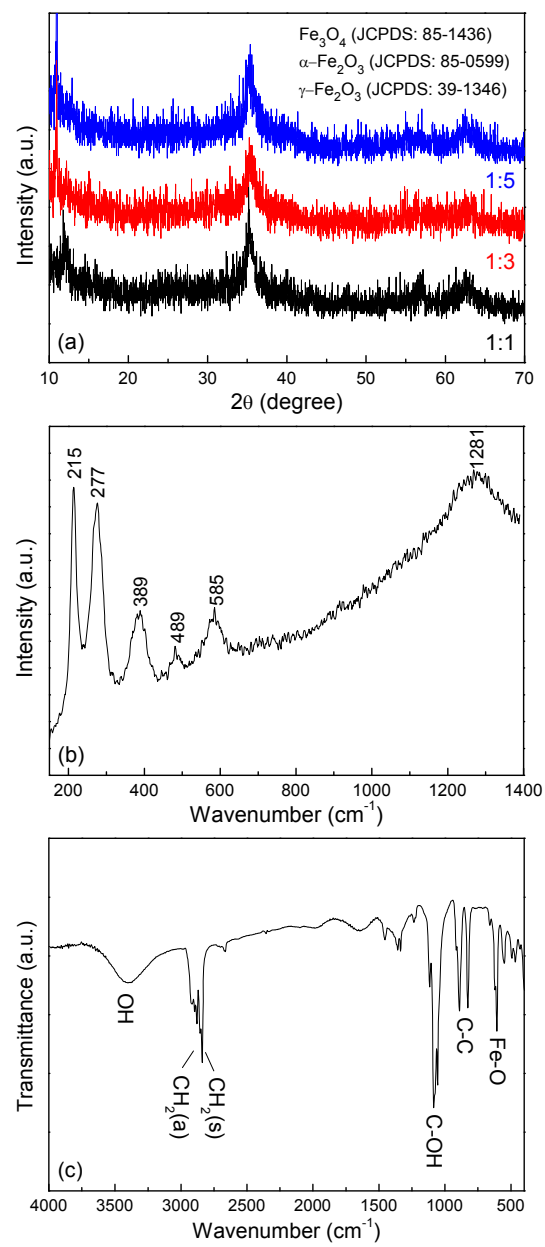


**Fig. 1.** (a) XRD patterns of 12 h-products with different $Fe^{2+}$/urea ratios. (b) Raman spectrum and (c) FTIR spectrum of the 12 h-product with $Fe^{2+}$/urea ratio of 1:1.